Smart Structures and Systems, *Vol. 33, No. 5 (2024) 325-332*
https://doi.org/10.12989/sss.2024.33.5.325

Carbonation depth prediction of concrete bridges based on long short-term memory

Youn Sang Cho [1a], Man Sung Kang [1b], Hyun Jun Jung [2c] and Yun-Kyu An*[1]

[1] *Department of Architectural Engineering, Sejong University 209 Neungdong-ro, Gwangjin-gu, Seoul, Republic of Korea*
[2] *Korea Authority of Land & Infrastructure Safety (KALIS), Jinju 52856, Republic of Korea*

(*Received September 7, 2023, Revised March 27, 2024, Accepted May 9, 2024*)

Abstract. This study proposes a novel long short-term memory (LSTM)-based approach for predicting carbonation depth, with the aim of enhancing the durability evaluation of concrete structures. Conventional carbonation depth prediction relies on statistical methodologies using carbonation influencing factors and in-situ carbonation depth data. However, applying in-situ data for predictive modeling faces challenges due to the lack of time-series data. To address this limitation, an LSTM-based carbonation depth prediction technique is proposed. First, training data are generated through random sampling from the distribution of carbonation velocity coefficients, which are calculated from in-situ carbonation depth data. Subsequently, a Bayesian theorem is applied to tailor the training data for each target bridge, which are depending on surrounding environmental conditions. Ultimately, the LSTM model predicts the time-dependent carbonation depth data for the target bridge. To examine the feasibility of this technique, a carbonation depth dataset from 3,960 in-situ bridges was used for training, and untrained time-series data from the Miho River bridge in the Republic of Korea were used for experimental validation. The results of the experimental validation demonstrate a significant reduction in prediction error from 8.19% to 1.75% compared with the conventional statistical method. Furthermore, the LSTM prediction result can be enhanced by sequentially updating the LSTM model using actual time-series measurement data.

Keywords: bridge; concrete carbonation; deep learning; long short-term memory; prediction; time-series update

1. Introduction

Structural durability is essential for ensuring a structure's resilience against damage, aging, and environmental factors (Ghanooni-Bagha *et al*. 2020, Chen *et al*. 2021). Evaluating durability involves several parameters such as chloride ion penetration (Loreto *et al*. 2012, Lei 2012), carbonation depth, quality of cover concrete, and other factors relevant to corrosive environments (Konečný *et al*. 2020). These parameters are combined to calculate the comprehensive durability ratio (Zheng and Lin 2012, Li 2019), aiding facility managers in devising effective maintenance plans to prevent structural collapse (Na *et al*. 2012). In the Republic of Korea, periodic durability assessments of civil infrastructures have been mandatory under the Special Act on Safety Control and Maintenance of Establishments law since 1995. Even though such as the collapse of the Jungja Bridge in the Republic of Korea recently collapsed due to inadequate durability estimation and insufficient maintenance repair. Carbonation depth prediction is an aspect of concrete structure durability assessment and is closely linked to concrete deterioration. Conventional methods for predicting carbonation depth mainly rely on statistical methods such as the Bayesian theorem or mathematical models (Zambon *et al*. 2018, Forsdyke and Lees 2023). For instance, Tasaka *et al*. (2009) employed the Bayesian theorem to enhance concrete carbonation depth prediction by incorporating measurement data, while Li and Zhou (2013) analyzed time-series carbonation depth data based on Fick's first law. These approaches commonly establish correlations between carbonation depth and velocity coefficient (Silva *et al*. 2014). However, they often struggle to adapt to new measurement data and may yield prediction results with wide confidence intervals. Extensive and precise data are typically required to ensure the accuracy of the statistical approaches, but, unfortunately, reliable time-series carbonation depth data obtained from a certain in-situ facility is quite limited. For instance, while the Republic of Korea's facility management system (FMS) has recorded mandatory assessment data for 28 years, only 51 bridges have reliable carbonation depth data containing more than three sequential samples in a specific bridge member. This limited dataset hinders the accuracy of the conventional predictions.

To address these technical limitations, this study proposes a novel technique that combines the Bayesian theorem with long short-term memory (LSTM) for carbonation prediction. The training dataset, comprising 99,191 in-situ concrete bridge carbonation depth data, was generated based on the Bayesian theorem, followed by the

*Corresponding author, Ph.D., Professor,
E-mail: yunkyuan@sejong.ac.kr
[a] Ph.D. Student, E-mail: lpnfx@sju.ac.kr
[b] Ph.D. Student
[c] Ph.D.

ISSN: 1738-1584 (Print), 1738-1991 (Online)

establishment of an LSTM model for carbonation depth prediction. This approach enhances prediction accuracy and reliability by continuously updating the prediction results with in-situ measurement data. The proposed carbonation depth prediction network is validated experimentally using carbonation depth data obtained from the Miho River bridge in the Republic of Korea.

The subsequent sections of this paper are organized as follows: Chapter 2 presents the development of bridge carbonation depth prediction based on the LSTM network. Chapter 3 discusses the experimental validation of the proposed technique. Finally, Chapters 4 and 5 provide the discussion and conclusion, respectively.

2. LSTM-based carbonation depth prediction model

LSTM networks excel in capturing temporal dependencies and adapting to changing patterns (Hochreiter and Schmidhuber 1997), making them ideal for predicting carbonation depth changing patterns in sequential data. The flow chart depicted in Fig. 1 illustrates the carbonation depth prediction process using the LSTM model. The process comprises two steps: (1) generation of training data and (2) prediction process based on the LSTM model. In Step (1), the training dataset is generated from the facility management system (FMS) data. Due to the limited availability of time-series carbonation depth data in FMS, a reliable training dataset was artificially generated using Bayesian theorem-based calculations of the carbonation velocity coefficient (A) and environmental condition-dependent carbonation depth data (gd_t). Subsequently, Bayesian-updated carbonation depth datasets (ud_t) are generated for each target bridge considering in-situ measurement data. ud_t is generated until the first measurement data, which serve as training data for the LSTM model. Once A, gd_t, and ud_t are generated, carbonation depth prediction using LSTM is conducted in Step (2). First, the LSTM input dataset (d_I) comprising the most recent arbitrary steps (n_1) from ud_t is prepared. Subsequently, the LSTM model is trained using ud_t specific to the target bridge. The trained LSTM model predicts the next steps (n_2) with d_I. The prediction results are compared with the bridge measurement data using the conditional statement in Fig. 1 to update d_I. If the conditional statement is met, the prediction proceeds; otherwise, it is terminated. The update of d_I adds $D_t{}^m$ to d_P for generating the dataset, which used as the next input (d_{I+i}) to the LSTM model.

Fig. 2 presents a typical carbonation depth prediction process by utilizing the LSTM model. Fig. 2(a) illustrates the representative A trends depending on various

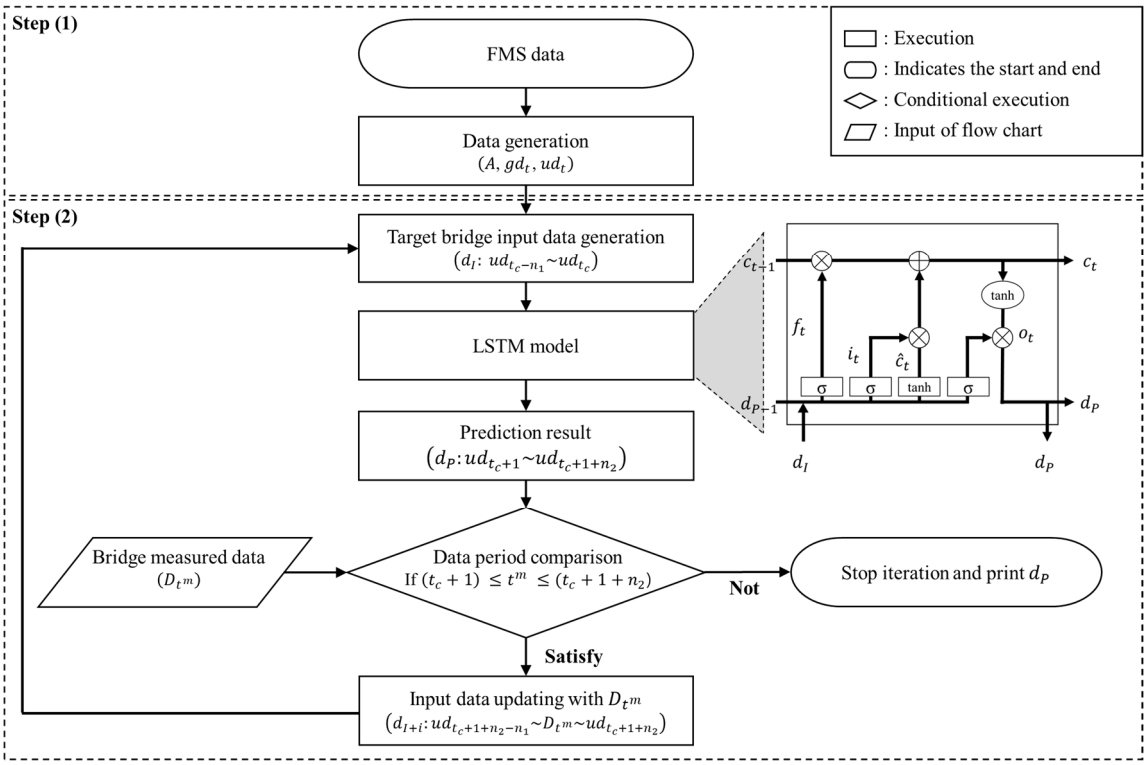

Fig. 1 Flow chart of carbonation depth prediction process using LSTM model: A is the carbonation velocity coefficient, gd_t and ud_t are generated carbonation depth data and Bayesian-updated carbonation depth data, t, t_c, and t^m are time of the carbonation depth data (year), current time, and the time of the measured data, d_I, d_p, and $D_t{}^m$ are input data, prediction result, and bridge measured carbonation depth data, n_1 and n_2 are the time step of the input data and the time step of the prediction result, c_t is cell state of the LSTM model, $\hat{c}_t$ is candidate value computed with input and hidden output data, f_t, i_t, and o_t are forget gate, input gate, and output gate of LSTM model, σ in the LSTM architecture is sigmoid function

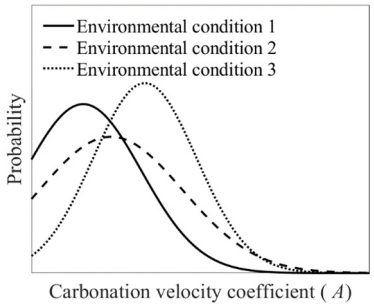

(a) Carbonation velocity coefficient distribution (A)

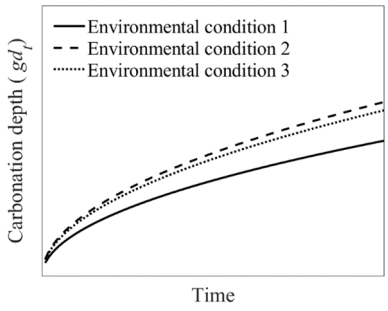

(b) Carbonation depth distribution (gd_t)

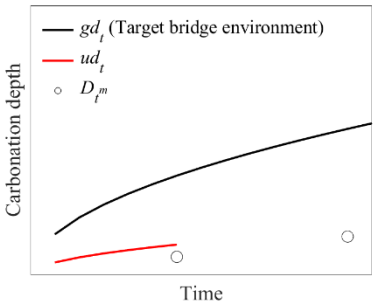

(c) gd_t selection and Bayesian updating

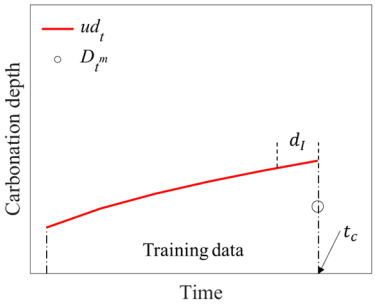

(d) LSTM model training and updating

Fig. 2 Carbonation depth data generation and LSTM updating: gd_t is the generated carbonation depth data. ud_t is the carbonation depth data updated with Bayesian theorem. D_t is the measurement carbonation depth data of a specific target bridge. d_I is the input data of LSTM model, and t_c is the current time

environmental conditions, which are calculated from the FMS dataset. gd_t is then computed from A, as depicted in Fig. 2(b). Next, a specific target bridge is chosen, and the corresponding gd_t is selected to compute ud_t by considering the environmental conditions of the target bridge. Fig. 2(c) compares the representative gd_t and ud_t obtained by using two $D_t{}^m$ points based on Bayesian theorem. In Fig. 2(d), the LSTM model is trained using ud_t, and a partial segment of ud_t up to t_c is utilized as d_I. This trained LSTM model employs d_I to predict carbonation depth in the next time step. When the prediction time step reaches to t_c, d_I is sequentially updated with $D_t{}^m$.

The subsequent sections elaborate on each procedure.

Step (1) Data generation: In FMS, there are 99,191 concrete carbonation depth data points corresponding to 37,775 bridges. However, only 9.77% of the carbonation depth data are available as time-series data in FMS dataset, covering 3,690 bridges. This insufficient data poses challenges in deriving meaningful analytical results for general bridges and effectively training the LSTM model. Therefore, more reliable time-series carbonation depth data are essential for LSTM model training. In this study, the Bayesian theorem is employed to generate representative bridge carbonation depth data, considering the influence of environmental conditions such as humidity and carbon dioxide (CO_2) rate (Monteiro *et al*. 2012, Liu *et al*. 2020). Thus, carbonation depth data are categorized based on environmental conditions.

To facilitate the sequential conversion of carbonation depth data for the LSTM model, it is essential to convert carbonation depth data to the velocity coefficient A. Notably, A remains unaffected by time and is only influenced by the bridge location. The carbonation rate, expressed in terms of carbonation depth data, adheres to Fick's first law and related equation (Jung 2010)

$$A = \sqrt{\frac{2D_{CO_2}}{a} \cdot C_a} = d_t/\sqrt{t} \tag{1}$$

where A is the carbonation velocity coefficient (mm/year$^{0.5}$). D_{CO_2} denotes the diffusion coefficient of CO_2, a is the amount of required CO_2 to carbonize a unit volume of concrete (mm^2/year), and C_a is the concentration of CO_2 in the atmosphere (mm^2/year). d_t is the carbonation depth (mm) at time t. The d_t is typically affected by environmental conditions such as CO_2 concentration, temperature, and humidity. These environmental effects are assumed to be correlated with target bridge locations such as urban, outside of urban, river, land, and sea. Therefore, d_t from FMS must be categorized by location to obtain A. Although, the bridge's location should be considered when converting A to d_t.

As illustrated in Fig. 3, d_t is categorized according to environmental locations such as rivers, land, and sea in urban areas or outside of urban areas. Table 1 summarizes the number of concrete bridges classified into six distinct locations.

The distributions of A are classified according to the environmental locations of the bridge and can be evaluated as follows

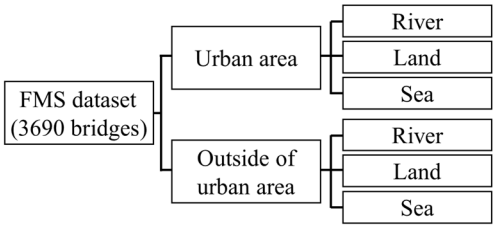

Fig. 3 Data categorization

Table 1 Number of concrete bridges classified into six distinct locations

Location	Number of bridges
River, urban area (RU)	514
Land, urban area (LU)	673
Sea, urban area (SU)	7
River, outside the urban area (ROU)	1,631
Land, outside an urban area (LOU)	780
Sea, outside the urban area (SOU)	85

$$N(A|\mu,{\sigma_A}^2) = \frac{1}{(2\pi{\sigma_A}^2)^{\frac{1}{2}}}\exp\{-\frac{1}{2{\sigma_A}^2}(A-\mu)^2\} \quad (2)$$

where μ and σ_A denote the mean value and standard deviation of A, respectively. The mean values and standard deviations of A with respect to the bridge locations are listed in Table 2.

The mean values of A in urban areas are greater than those observed outside urban areas. Notably, bridges located in SU have maximum mean values of A. However, from the set of bridges in outside of urban area, LOU exhibited the maximum mean values. Based on Eq. (2), Gaussian distributions of A differ according to the environmental context, as shown in Fig. 4(a). Here, the representative 100 years carbonation depth data are displayed in Fig. 4(b).

Once distributions of A are obtained, the corresponding gd_t can be computed using Eq. (1), as shown in Fig. 4(b). The representative value of A was selected to generate the distribution of d_t according to the location. To effectively train the LSTM model, the input d_t should be indicated in

Table 2 μ and σ of the carbonation velocity coefficient

Location	Mean (μ)	Standard deviation (σ)
RU	2.450	2.747
LU	3.762	1.405
SU	5.366	2.443
ROU	2.255	2.391
LOU	2.899	2.380
SOU	2.761	1.920

a sequential format. First, the location of the representative bridge is selected for subsequent training and prediction procedures. Both ${D_t}^m$ and gd_t from the target bridge are used to generate training and input data for updating the LSTM model. gd_t is chosen based on the same location as the target bridge. Both ${D_t}^m$ and gd_t from the target bridge are used for the Bayesian theorem. gd_t of the location is updated with ${D_t}^m$ from the target bridge using the Bayesian theorem (Jung *et al*. 2020)

$$P_1(A) = c_1 P(D|A)\cdot P_0(A) \quad (3)$$

where $P_0(A)$ and $P_1(A)$ are the prior and posterior probabilities of uncertainties in the carbonation velocity coefficient probability, D is the measured concrete carbonation data from the target bridge, $P(D|A)$ is a likelihood function that represents the uncertainties in D when the variable A is the carbonation velocity coefficient, and c_1 is a constant determined by the previous probability conditions. Subsequently, the likelihood function for the Bayesian theorem is computed by the following equation

$$p_k = \exp\left[-\sum_t \frac{1}{2}\left(\frac{D_t - gd_t^k}{\sigma_t}\right)^2\right] \quad (4)$$

where D_t is the measured carbonation depth data from the target bridge, gd_t^k is the generated time-series carbonation depth data. k is the number of randomly sampled A and σ_t is the standard deviation of existing experimental values at measured time t. The division of the A distribution into k bins uses less in-situ measured data and less time based on the Latin hypercube sampling method (Jung and Kim 2010). Random sampling is performed by dividing into k

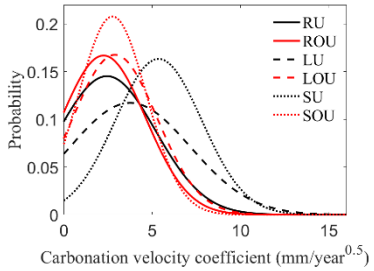

(a) Generated carbonation velocity coefficient distribution

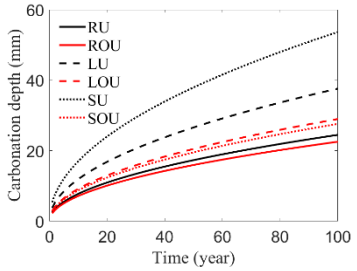

(b) Generated carbonation depth distribution

Fig. 4 Carbonation depth data generation procedure: River, urban area (RU), Land, urban area (LU), and Sea, urban area (SU) are the river, land, and sea in the urban area, and River outside the urban area (ROU), Land outside an urban area (LOU), and Sea outside the urban area (SOU) are the river, land, and sea outside the urban area

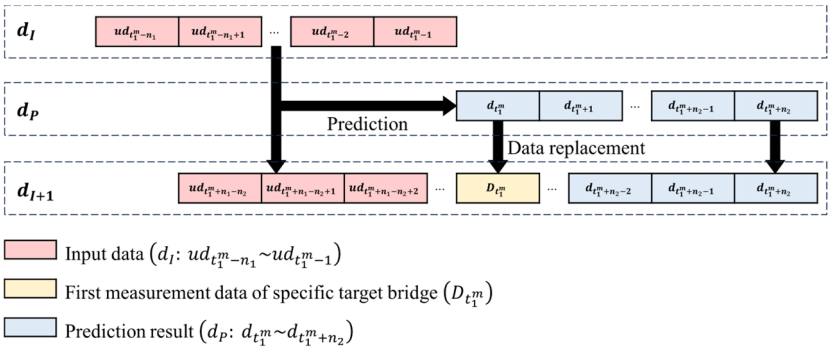

Fig. 5 LSTM model prediction and d_I updating: t_1^m is the point of the first measurement data, n_1 and n_2 are steps of the d_I and d_P, d_{I+1} is the updated input data

intervals of equal probability. The extracted A values through random sampling are plugged into Eq. (1) to compute gd_t^k, which is then used in Eq. (4). The carbonation depth data are multiplied by the likelihood function that reflects the in-situ estimated data. The updated data are generated by the equation

$$ud_t = \sum_k P_1(D_t^k) gd_t^k = c_0 \sum_k p_k \, gd_t^k \tag{5}$$

where ud_t is the mean value of the updated carbonation depth data, and c_0 is the reciprocal number of the sum of p_k. ud_t was updated using the Bayesian theorem, which is conventionally used in carbonation depth prediction. The conventional carbonation depth prediction method relies on the Bayesian theorem resulting in a dynamically evolving intrinsic slope with each update based on newly measured data. The conventional prediction method uses the Bayesian theorem, which generates prediction results by changing the intrinsic slope in each update. However, the LSTM model produces real-time prediction results that adapt to newly measured data. Therefore, ud_t was used for training the LSTM model.

Step (2) LSTM model training and carbonation depth prediction based on the trained LSTM model: Upon the generation of ud_t specific to the target bridge, the preceding ud_t data points before the initial measured data of the in-situ bridge are employed for training purposes. Therefore, the LSTM model is used separately according to the target bridge.

The part of ud_t used for training data is shown in Fig. 5. The LSTM model is trained with the ud_0~$ud_{t_1^m-1}$. In the architecture of the LSTM model shown in Fig. 1, the path of the cell state (c_t) incorporates information from previous data points. The other path of the d_p oversees new input data and outputs predictions accordingly. The candidate value $(\hat{c}_t)$ is obtained by applying a hyperbolic tangent to the sum of d_I and d_{P-1}. The forget gate f_t generates the value by applying the sigmoid function to the sum of d_I and d_{P-1}. The input gate i_t multiplies the values of f_t and $\hat{c}_t$. c_{t-1} is updated with the output of the forget and input gates. The output gate o_t generates d_p by multiplying the hyperbolic tangent applied c_t by the output value of f_t. Sequential d_p generated by repeating Step (2) is the prediction result based on the LSTM model. In the case of the LSTM model training, d_I in the architecture of the LSTM is a first n_1 steps of ud_t, and the first d_p in the architecture of the LSTM is (n_1+1)~(n_1+1+n_2) of ud_t.

The trained LSTM model is used to obtain prediction results from the input data. A detailed description of the prediction procedure is as follows: The prediction is performed in four steps. The input data consists of n_1 time steps (d_{I_1}) is passed through the trained LSTM model. The prediction result of d_{I_1} (d_{P_1}) is compared with the first measured data $(D_{t_1^m})$ using the conditional statement in Step (2). The predicted carbonation depth data in d_{P_1} simultaneously as $D_{t_1^m}$ is replaced with $D_{t_1^m}$ if the conditional statement is satisfied. The next input data (d_{I_2}) is generated with the combined data of d_{I_1} and d_{P_1} by excluding the preceding time points to align d_{I_2} with the length of n_1. The process is repeated, acquiring sequential prediction results from the LSTM model with each progression.

3. Experimental validation

The proposed LSTM-based carbonation depth prediction was experimentally validated using in-situ carbonation depth data from the Miho River bridge. Notably, the experimental validation data were not trained in the proposed LSTM model.

The characteristics of the Miho River bridge are summarized in Table 3. The Miho River bridge is located in Chungcheong Buk-do, Republic of Korea, and is 34 km away from urban areas, which is outside the urban area (ROU). Therefore, gd_t of ROU from FMS was used for data generation. The Miho River bridge was built in 1993 and has a length of 430 m, a width of 16.7 m, and a road width of 16 m. It has nine spans, with a maximum span length of 50 m. A bridge with a design load of DB-24 can support a maximum total weight of 43.2 tons (KDS 21 45). The bridge superstructure is a Prestressed Concrete (PSC) box girder, and the substructure is composed of T-shaped piers.

Table 3 Characteristics of the Miho River bridge

Characteristic	Details
Location	Chungcheongbuk-do (ROU)
Length	430 m
Width	16.7 m
Road width	16 m
Number of spans	9
Maximum span length	50 m
Designed load	DB-24
Construction year	1993
Superstructure type	Prestressed concrete (PSC) box

Table 4 D_{t^m} of Miho River bridge

t^m (year)	D_{t^m} (mm)
10	8.4
17	13.7
20	14.9

Step (1) Data generation in the Miho River bridge case: The carbonation depth data is affected based on the locations of the bridge, and its A can be obtained using Eq. (2). gd_t of ROU related to the Miho River bridge was obtained using representative A distributions mentioned in Fig. 4(a). The value of k in Eq. (4) is set to 9 in this study. Nine samples from A distribution of ROU were selected at a constant interval based on μ, given that the Miho River is located in ROU. Subsequently, Eq. (1) is applied to generate gd_t of ROU using the extracted A values. Additionally, gd_t is generated using nine representative carbonation velocity coefficients specific to ROU. This ensures that the carbonation depth data includes the characteristics of ROU. Furthermore, gd_t undergoes Bayesian updating with D_{t^m} of the Miho River bridge, as shown in Table 4.

The Miho River bridge is chosen as a validation example because it has three measurement data, which is the most data available within FMS. The carbonation depth in the Miho River bridge was measured 10, 17, and 20 years after bridge construction. D_{t^m} of the Miho River bridge are 8.4, 13.7, and 14.9 mm, respectively. After computinggd_ts of ROU, Eq. (4) is used to obtain p_k value from D_{t^m} and gd_ts of the Miho River bridge. The Bayesian updated ud_t is the carbonation depth data, which not only includes the characteristics of ROU but also the trend of D_{t^m} of Miho River bridge.

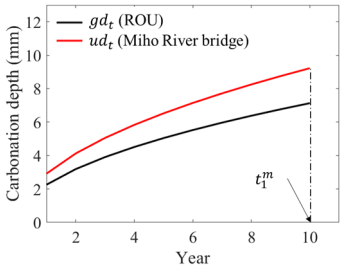

Fig. 6 Training data of Miho River bridge

Step (2) Training the LSTM model and prediction based on the Miho River bridge case: gd_t was updated by incorporating D_{t^m} from the Miho River bridge through a process of generating ud_t. D_{10} and D_{17} were used to update gd_t of ROU based on Bayesian theorem, resulting in ud_t which is defined as the conventional prediction result, $d_P^{(a)}$. Then, ud_t until D_{10} was used as a training data, also D_{10} and D_{17} were used for LSTM model updating. D_{20} was used as ground truth for validating the LSTM prediction results ($d_P^{(b)}$) as well as $d_P^{(a)}$.

Fig. 6 shows gd_t for ROU and ud_t for the LSTM model training. In this study, ud_t was generated to represent monthly data, derived from the training procedure of the LSTM model, utilizing the dataset up to the initial measured data point. To ensure precise prediction of carbonation depth, the dataset comprises 24 input sets corresponding to a temporal period of 2 years, along with 1 prediction set corresponding to a temporal period of 1 month. Therefore, for the Miho River bridge case, n_1 and n_2 in the prediction flow chart are set to 24 and 1, respectively. The interval d_I, extracted from ud_t covers 7 years and 11 months to 9 years and 11 months. This specific

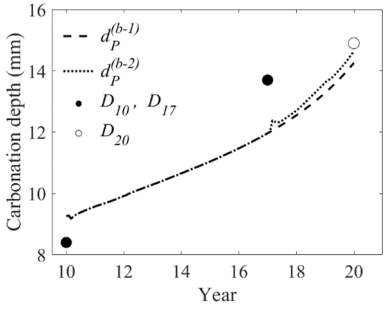

(a) $d_P^{(b-1)}$ and $d_P^{(b-2)}$

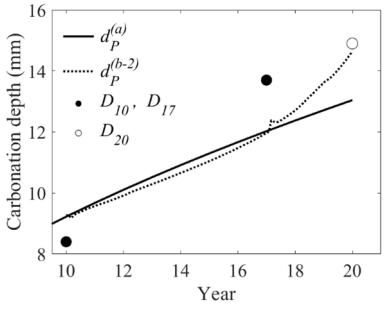

(b) $d_P^{(a)}$ and $d_P^{(b-2)}$

Fig. 7 Prediction results of the LSTM model: $d_P^{(b-1)}$ and $d_P^{(b-2)}$ are the prediction results of the trained LSTM model that was updated with the Miho River bridge's measurement data, D_{10} and D_{17}. D_{20} is also in-situ measurement data for validation. $d_P^{(a)}$ is the prediction result of the conventional method

Table 5 Miho River bridge validation results

	D_{20}	$d_P^{(a)}$	$d_P^{(b-1)}$	$d_P^{(b-2)}$
Carbonation depth (mm)	14.9	13.679	14.257	14.639
Error (mm)	-	1.221	0.643	0.261
Error (%)	-	8.19	4.31	1.75

time frame is selected due to the use of D_{10} for updating the LSTM model. Consequently, the first d_P satisfies the update conditional statement shown in Fig. 1, triggering the subsequent updating process using the measurement data to generate d_{I+1}.

To ensure precise prediction of carbonation depth, the dataset comprises 24 input sets corresponding to a temporal period of 2 years, along with 1 prediction set corresponding to a temporal period of 1 month. Consequently, for the Miho River bridge case, n_1 and n_2 in the prediction flow chart are 24 and 1, respectively. d_I covers from 7 years 11 months to 9 years and 11 months.

Fig. 7(a) shows $d_P^{(b)}$ marked as a broken line from 10 to 20 years. $d_P^{(b-1)}$ in Fig. 7(a) represents the prediction result of the LSTM model solely updated with D_{10}. $d_P^{(b-2)}$ represents the prediction one updated using both D_{10} and D_{17}. Notably, $d_P^{(b-2)}$ closely aligns with D_{20}. Fig. 7(b) compares the results of $d_P^{(a)}$, representing a Bayesian theorem-based conventional prediction method (Jung *et al.* 2020), and $d_P^{(b-2)}$. The comparison demonstrates that $d_P^{(b-2)}$ is more closely aligned to D_{20} than $d_P^{(a)}$. Here, $d_P^{(b-1)}$ shows the small heap right after updating with D_{10}, and $d_P^{(b-2)}$ has similar but opposite directional small heap after updating with D_{17}. These heap phenomena caused by the discrepancy between d_I and $D_t{}^m$ used to update the LSTM model. If d_I exactly matches with $D_t{}^m$, the prediction result follows the trained data trend without heap. The higher $D_t{}^m$ than d_I makes upward heap, and lower $D_t{}^m$ produces downward heap. One more interesting thing to see here is that the prediction curve trend is changed after the heap phenomenon. Since the network is updated with different $D_t{}^m$ from d_I, it is speculated that it tries to compensate the gap arised from the heap. In Fig. 7 (a), the downward heap appears at 10 years due to the lower D_{10} than the initial d_I, and the gradient of $d_P^{(b-1)}$ is adjusted. Compared with the trend of d_I which has 2 years-time unit in this study, the gradient of $d_P^{(b-1)}$ is gradually increased. Such rising tendency is amplified along the time step if there is no more update with $D_t{}^m$. Similar phenomenon can be seen at 17 years. $d_P^{(b-2)}$ is suddenly upward with the heap caused by D_{17}, and the rising tendency is weakened after 17 years. In conclusion, it is worthy noted that $d_P^{(b-2)}$ updated with D_{17} shows the result closer to D_{20} than $d_P^{(b-1)}$ as well as $d_P^{(a)}$.The accuracy of the prediction data was evaluated based on the error of the prediction results compared with D_{20}. The error was computed using the following equation

$$Error = \frac{|x - x_i|}{x} \cdot 100\ (\%) \tag{8}$$

where x_i and x are the prediction result and ground truth, respectively.

Table 5 presents a comprehensive overview of the errors of $d_P^{(b)}$ derived from the LSTM model, showcasing their superiority over the $d_P^{(a)}$. Notably, it is evident that the errors of $d_P^{(b)}$ are reduced from 4.31% to 1.75% through sequential LSTM model updating. Specifically, the error of $d_P^{(a)}$ stands at 1.221 mm, whereas $d_P^{(b-1)}$ and $d_P^{(b-2)}$ show errors of 0.643 and 0.261, respectively. This indicates a substantial reduction in error, with $d_P^{(b-1)}$ showcasing a decrease of 47.36% compared with $d_P^{(a)}$. Moreover, $d_P^{(b-2)}$ exhibits a remarkable reduction in error by 78.60% when compared with $d_P^{(a)}$. In summary, the error decreased when an update was performed.

4. Discussion

The conventional method for carbonation prediction lacks the capability to consider each bridge's conditions. On the other hand, the LSTM-based carbonation depth prediction relies on $D_t{}^m$ and demonstrates higher prediction accuracy due to its updating ability, which adaptively incorporates a recent $D_t{}^m$. The experimental validation results show that prediction errors can be decreased as the number of updating is increased with in-situ measurement data. This suggests that more frequent updates of the predictive network are able to achieve higher prediction accuracy.

One limitation of d_t is only few of data in FMS datasets that satisfy an ascending trend and at least three data points. Although, gd_t is generated from A, which is depending on environmental locations (RU, LU, SU, ROU, LOU, and SOU), ud_t computed using Bayesian updating may not be perfectly tailored for a specific target bridge. If more time-series data can be cumulated in each target bridge, the prediction accuracy can be improved.

Future research will explore additional bridges under diverse environmental conditions. As this study relied on a limited FMS dataset for d_t, the model's utility with LSTM is expected to expand with the inclusion of more data. Moreover, the enhancement in prediction accuracy through successive updates to the LSTM model is evident from the comparison of $d_P^{(b)}$. Therefore, the LSTM model's performance can be further improved with additional data accumulation. While this study primarily focused on carbonation depth data, other factors such as chloride accumulation and concrete strength should be included to validate the proposed model. Additionally, other types of infrastructure such as tunnels, dams, and sewage facilities warrant consideration. Furthermore, since measurement of durability data are human-generated rather than sensor-based, further research is needed to develop a filtering process to determine the reliability of measurement data.

5. Conclusions

This study proposed an LSTM-based method for predicting carbonation depth, offering a valuable approach for evaluating the durability of concrete bridges. Departing from a stand-alone LSTM approach, we applied the Bayesian theorem to data generation, effectively augmenting insufficient data to train the LSTM model.

The effectiveness of the proposed method was compared with a conventional method using in-situ bridge carbonation depth data. Using the Miho River bridge in the Republic of Korea as a case study, this study affirm that the trained LSTM model can generate more reasonable prediction results than the conventional method using measured carbonation depth data. However, given that this study was confined to a specific target bridge, further validation across different locations, beyond ROU settings, is imperative.

The proposed method holds promise for enhancing concrete bridge management practices, with potential applications extending to durability assessment, residual life estimation, and life cycle cost estimation.

Acknowledgments

This study was supported by the BK21 FOUR (Fostering Outstanding Universities for Research, No. 412024115147) funded by the Ministry of Education (MOE, Korea) and National Research Foundation of Korea (NRF), and Ministry of the Interior and Safety as Human Resource Development Project in Earthquake Disaster Management.

References

Chen, G., Lv, Y., Zhang, Y. and Yang, M. (2021), "Carbonation depth predictions in concrete structures under changing climate condition in China", *Eng. Fail. Anal.*, **119**, 104990. https://doi.org/10.1016/j.engfailanal.2020.104990

Ghanooni-Bagha, M., YekeFallah, M.R. and Shayanfar, M.A. (2020), "Durability of RC structures against carbonation-induced corrosion under the impact of climate change", *KSCE J. Civil Eng.*, **24**(1), 131-142. https://doi.org/10.1007/s12205-020-0793-8

Hochreiter, S. and Schmidhuber, J. (1997), "Long short-term memory", *Neural Computat.*, **9**(8), 1735-1780. https://doi.org/10.1162/neco.1997.9.8.1735

Forsdyke, J.C. and Lees, J.M. (2023), "Model fitting to concrete carbonation data with non-zero initial carbonation depth", *Mater. Struct.*, **56**(1), 22. https://doi.org/10.1617/s11527-023-02104-0

Jung, H. (2010), "Durability analysis and development of probability-based carbonation prediction model in concrete structure", *KSCE J. Civil Environ. Eng. Res.*, **30**(4A), 343-352. https://doi.org/10.12652/Ksce.2010.30.4A.343

Jung, H.J. and Kim, G.S. (2010), "A long-term durability prediction for RC structures exposed to carbonation using probabilistic approach", *J. Korea Inst. Struct. Maint. Inspect.* (*KSMI*), **14**(5), 119-127. https://doi.org/10.11112/jksmi.2010.14.5.119

Jung, H., Im, S.B. and An, Y.K. (2020), "Probability-based concrete carbonation prediction using on-site data", *Appl. Sci.*, **10**(12), 4330. https://doi.org/10.3390/app10124330

Konečný, P., Lehner, P., Vořechovská, D., Šomodíková, M., Horňáková, M. and Rovnaníková, P. (2020), "Extended evaluation of durability-related field inspection data from concrete bridges under service", *Procedia Struct. Integr.*, **26**, 430-438. https://doi.org/10.1016/j.prostr.2020.06.054

KDS 21, 45 (2022), Hypothesis Bridge and Pavement Dual Design Standards, Korea Construction Standards Center, Republic of Korea. [In Korean]

Lei, J.Q. (2012), "Research on durability of coastal concrete bridges", *Adv. Mater. Res.*, **374-377**, 2167-2170. https://doi.org/10.4028/www.scientific.net/AMR.374-377.2167

Li, S. (2019), "Durability evaluation of concrete bridges considering multi-scale high-efficiency numerical models", In: *2019 International Conference on Smart Grid and Electrical Automation* (*ICSGEA*), pp. 169-172. https://doi.org/10.1109/ICSGEA.2019.00046

Li, G.Z. and Zhou, X.G. (2013), "The research of predicting the carbonation depth of concrete with time-series analysis", *Appl. Mech. Mater.*, **351-352**, 1694-1699. https://doi.org/10.4028/www.scientific.net/AMM.351-352.1694

Liu, P., Yu, Z. and Chen, Y. (2020), "Carbonation depth model and carbonated acceleration rate of concrete under different environment", *Cement Concrete Compos.*, **114**, 103736. https://doi.org/10.1016/j.cemconcomp.2020.103736

Loreto, G., Di Benedetti, M. and Nanni, A. (2012), "Evaluation of concrete structures in marine environment: Geiger key bridge", *Nondestructive Characterization for Composite Materials*, *Aerospace Engineering*, *Civil Infrastructure*, *and Homeland Security*, **8347**, 555-562. https://doi.org/10.1117/12.914862

Monteiro, I., Branco, F.A., de Brito, J. and Neves, R. (2012), "Statistical analysis of the carbonation coefficient in open air concrete structures", *Constr. Build. Mater.*, **29**, 263-269. https://doi.org/10.1016/j.conbuildmat.2011.10.028

Na, U.J., Kwon, S.J., Chaudhuri, S.R. and Shinozuka, M. (2012), "Stochastic model for service life prediction of RC structures exposed to carbonation using random field simulation", *KSCE J. Civil Eng.*, **16**(1), 133-143. https://doi.org/10.1007/s12205-012-1248-7

Silva, A., Neves, R. and De Brito, J. (2014), "Statistical modelling of carbonation in reinforced concrete", *Cement Concrete Compos.*, **50**, 73-81. https://doi.org/10.1016/j.cemconcomp.2013.12.001

Tasaka, S., Shinozuka, M., Chaudhuri, S.R.A.Y. and Na, U.J. (2009), "Bayesian inference for prediction of carbonation depth of concrete using MCMC", *Mem Akashi Tech Coll*, **52**, 45-50.

Zambon, I., Vidovic, A., Strauss, A., Matos, J. and Friedl, N. (2018), "Prediction of the remaining service life of existing concrete bridges in infrastructural networks based on carbonation and chloride ingress", *Smart Struct. Syst., Int. J.*, **21**(3), 305-320. https://doi.org/10.12989/sss.2018.21.3.305

Zheng, X.Z. and Lin, J.F. (2012), "Pre-evaluation of durability for concrete bridge", *Adv. Mater. Res.*, **594-597**, 1581-1585. https://doi.org/10.4028/www.scientific.net/AMR.594-597.1581